Pramāṇa – J. Phys., Vol. 27, Nos 1 & 2, July & August 1986, pp. 275–290.

Study of the K_α satellites and hypersatellites in the x-ray and Auger spectra of neon

LAKSHMI NATARAJAN, A V TANKHIWALE and C MANDE
Department of Physics, Nagpur University, Nagpur 440010, India

Abstract. We report in this paper our calculations of the energies of the satellite and hypersatellite lines in the x-ray and Auger spectra of neon, using screened hydrogenic wavefunctions. Our calculations have enabled us to draw an energy level diagram for the neon atom in various defect-electron configurations. It is possible to show the transitions giving rise to the various x-ray and Auger satellites and hypersatellites using this diagram.

Keywords. X-ray spectra; Auger spectra; satellite lines; hypersatellite lines; defect-electron configurations; spectator vacancies, relaxed-core approximation.

PACS No. 32·20; 32·80

1. Introduction

Professor M N Saha's immense contributions in the field of thermal atomic ionization (Saha 1920, 1921; Saha and Banerji 1931) are well known. His illustrious student Dr D S Kothari further extended this work (Kothari and Majumdar 1929) to the study of stellar physics. Due to the high temperatures existing in the stars, the atoms collide with each other with great speeds causing multiple ionization in the outer shells of the atom. Thermal energies of the atoms, being of the order of a few eV, are sufficient enough to ionize the atoms in their outer shells because the electrons in them are loosely bound. However, the binding energies of the electrons in the inner atomic shells are of the order of a few keVs. Thus the inner shells usually remain unscathed by the process of thermal ionization. We would like to pay in this paper our humble tributes to Prof. D S Kothari, whose work has brought laurels to India. We have made an attempt to extend the work of outer shell atomic ionization to the study of multiple ionization in the inner shells of atoms, occurring due to different processes. Natural processes like β decay, orbital electron capture and internal conversion (Emery 1975; Krause 1973; Crasemann 1975; Fink *et al* 1973) lead to multiple ionization of inner shells as a result of the shake-off phenomenon (Carlson *et al* 1968). Multiple inner shell ionization in target atoms can also be produced by using high energy photons, electrons, protons etc possessing energies of the order of a few meV as projectiles. With the development in the last few years of high energy heavy ion accelerators, a large number of experiments (Richard *et al* 1973; Briand *et al* 1971; Sagawa 1971; Fink *et al* 1973; Åberg and Suvanen 1982) on heavy ion-atom collisions have been performed.

The atoms with multiple ionization produced in the inner shells are often called exotic atoms. Such an atom deexcites itself mainly by two independent competing

---

The authors felicitate Prof. D S Kothari on his eightieth birthday and dedicate this paper to him on this occasion.

processes (i) the radiative transition wherein an electron from a higher shell jumps to the inner shell in the presence of spectator vacancies, giving rise to the x-ray satellite and hypersatellite lines lying on the high energy side of the corresponding diagram line and (ii) radiationless transitions leading to the emission of the satellite and hypersatellite lines in Auger spectra, which lie chiefly on the low energy side of the diagram Auger line (Burch *et al* 1972).

The fascinating and the complex subject of x-ray satellites has aroused the interest of workers since the time of Siegbahn (1925) and a great deal of experimental and theoretical work has been done in this field (Hirsh 1942; Deodhar 1962; Sachenko and Demekhin 1966; Åberg 1967). The experimental work on enhanced x-ray fluorescence yields in the violent heavy ion-atom collisions, leading to the occurrence of satellites and hypersatellites due to single and double ionization of the K shell and multiple ionization of the L shell, has been reviewed by workers like Richard (1975) etc. Considerable theoretical calculations on this subject have been done by Bhalla *et al* (1973).

The Auger electron spectra were initially regarded as a 'nuisance effect'. In course of time, Auger spectroscopy found very wide applications in atomic and nuclear physics, surface studies, chemical physics etc. Work on Auger spectroscopy has been reviewed by Burhop and Asaad (1972) and Bambynek *et al* (1972). The emission of Auger satellite and hypersatellite lines in the heavy ion-atom collisions has been studied amongst others by Ogurtsov (1972), Rudd and Macek (1972), Burch (1973), McGuire (1975) and Garcia *et al* (1973). Some experiments on measurements of transition energies and transition rates have been made by Krause *et al* (1970) and Matthews *et al* (1973), while theoretical calculations have been carried out by Bhalla *et al* (1973).

In the present paper, making use of screened hydrogenic wavefunctions, we have made an attempt to draw an energy level diagram for neon, a typical light atom, in various defect electron configurations, which would show the transitions giving rise to the x-ray satellite and hypersatellite lines. An attempt has similarly been made to calculate the energies of the satellite and hypersatellite lines of neon in the Auger spectra to study the different transient atomic states and to give proper assignments to the Auger satellites and hypersatellites. We have particularly chosen neon for the following reasons: (i) neon, being a closed shell inert element, forms a suitable system for investigations, since the experimental results are free from perturbing environmental effects, (ii) it is available as a gaseous target so that solid state effects are avoided, (iii) being a light atom, the approximation of LS coupling used is valid and (iv) considerable experimental and theoretical data are available for comparison for this element.

2. Procedure for calculations of configurational energies

For calculations of the energies of the satellite and hypersatellite lines, one needs the values of the average energies of the atom in various defect electron configurations. We have calculated these values making use of screened hydrogenic wavefunctions (Tankhiwale and Mande 1970; Lakshmi Natarajan *et al* 1986), neglecting configuration interactions. We have shown earlier (Tankhiwale *et al* 1971) that these screened hydrogenic wavefunctions, though somewhat deviating from the HFS wavefunctions of Herman and Skillman (1963) for the outer orbitals, agree very closely with

the HFS wavefunctions for the inner orbitals like 1*s*, 2*s*, 2*p* etc which are involved in the present calculations. Here the integrals involved come in a closed form because of their analytical nature and give a better picture of the processes occurring. The effective charges for different orbitals were obtained using the procedure given earlier (Lakshmi Natarajan *et al* 1986). The numerical values of Z_{eff} thus calculated for the neutral neon atom came out to be 9·64, 7·50 and 6·63 for the 1*s*, 2*s* and 2*p* orbitals respectively. Following the method of Tankhiwale *et al* (1971), the screening produced by each electron in the *K* and *L* shells on the other electrons is determined. For neon, our present calculation shows that the screening of a *K* shell electron by the other electron from the same shell is 0·36, while the screening for an *L* electron by a single *K* electron and a single *L* electron is 0·75 and 0·27 respectively.

In the non-relativistic framework, two alternative approaches (Larkins 1971a, b) can be used to calculate the average energies of the neutral and exotic atom. If the removal or transition involving an electron is rapid, such that the spectator electrons of the system are unable to readjust to the changing electron environment within the lifetime of the process, then the same radial wavefunctions may be used to represent the electrons of the system in both the initial and final states. This is the so-called 'sudden model' or 'frozen-core approximation model'. However, if the spectator electrons of the system are able to readjust to the changing electron environment during the lifetime of the transition process, the radial wavefunctions involving the different Z_{eff} values in the initial and final state of the atom have to be used. This is the 'adiabatic model' or the 'relaxed core approximation'. Following Larkins (1971a) and Bhalla *et al* (1973) we have followed the latter approximation because the atomic relaxation times ($\simeq$ 1 atomic time unit $= 2{\cdot}42 \times 10^{-17}$ sec) are known to be (Bambynek *et al* 1972) shorter than the lifetimes of the inner shell holes.

In the case of a light atom like neon, assuming that the Russel-Saunders coupling (Condon and Shortley 1977) holds true, the average energies of the neutral or exotic atom can be calculated using the following approximation due to Slater (1960)

$$E_{\text{average}} = \sum_{nl} I(nl) + \Sigma_{(\text{pairs})} \text{ interaction energies.} \tag{1}$$

Here $I(nl)$ is the one-electron integral term arising from the kinetic energy of the electron in the subshell *nl*, together with its electrostatic interaction energy with the nucleus. The interaction energies of various electron pairs are given in terms of the Coulomb and exchange integrals between the pairs of electrons in various subshells. These integrals, often called the Slater-Condon parameters, are given by the formulae

$$F^k(n_1l_1, n_2l_2) = e^2 \int_{r_1=0}^{\infty} \int_{r_2=0}^{\infty} R^2_{n_1l_1}(r_1) \times R^2_{n_2l_2}(r_2) \frac{(r_<)^k}{(r_>)^{k+1}} r_1^2 r_2^2 \, dr_1 \, dr_2 \tag{2}$$

and

$$G^k(n_1l_1, n_2l_2) = e^2 \int_{r_1=0}^{\infty} \int_{r_2=0}^{\infty} R_{n_1l_1}(r_1) \times R_{n_2l_2}(r_1) \frac{(r_<)^k}{(r_>)^{k+1}} R_{n_1l_1}(r_2) R_{n_2l_2}(r_2) r_1^2 r_2^2 \, dr_1 \, dr_2, \tag{3}$$

where $R_{n_1 l_1}$ and $R_{n_2 l_2}$ are the radial parts of the hydrogenic wavefunctions. Here $n_1 l_1$ and $n_2 l_2$ refer to the orbitals to which the two electrons belong.

To evaluate the Slater-Condon parameters F's and G's involving the 1*s*, 2*s* and 2*p* orbitals for neon, we have used the normalized hydrogenic radial wavefunctions R_{1s}, R_{2s} and R_{2p} containing the screening parameters determined by us. As in the earlier paper (Lakshmi Natarajan *et al* 1986) they are orthogonalized by the Schmidt orthogonalization process to yield the orthonormal set R_{1s}, R'_{2s}, R_{2p} which are then found to be similar in form to the wavefunctions of Morse *et al* (1935), though the constants and coefficients in them are different because of the different Z_{eff} values used by us. Using our Z_{eff} values, we have calculated the values of the one electron integrals $I(nl)$ and the F's and G's making use of the tables of Morse *et al* as given by Slater (1960).

3. Calculations of transition energies

3.1 *X-ray satellite and hypersatellite energies*

For neon, in the normal or exotic state, we write the electronic configuration as $1s^l 2s^m 2p^n$, where l, m and n denote the occupation numbers of electrons in the shells 1*s*, 2*s* and 2*p* respectively. The values of l and m vary from 0 to 2 and of n from 0 to 6. Then for the configuration $1s^l 2s^m 2p^n$, the average energy is given as

$$E_{\text{av}}(1s^l 2s^m 2p^n) = l\,I(1s) + m\,I(2s) + n\,I(2p)$$
$$+ \frac{l(l-1)}{2} E(1s, 1s) + \frac{m(m-1)}{2} E(2s, 2s) + \frac{n(n-1)}{2} E(2p, 2p)$$
$$+ lm\,E(1s, 2s) + ln\,E(1s, 2p) + mn\,E(2s, 2p). \tag{4}$$

Here E's are the interaction energies of the electron pairs and are expressed in terms of F's and G's.

For x-ray satellite and hypersatellite lines, the electric dipole selection rule permits only the 2*p* electron to go to the vacant 1*s* shell in the initial defect electron configuration. The initial and final state configurations are respectively $1s^l 2s^m 2p^n$ and $1s^{l+1} 2s^m 2p^{n-1}$, with m taking the values of 0 to 2 and n of 1 to 5. For a satellite line, $l = 1$, whereas $l = 0$ for a hypersatellite. It may be remembered that for the emission of a satellite or a hypersatellite there is at least one spectator vacancy in the 2*s* or 2*p* shell initially. The energies of the x-ray satellite and hypersatellite lines are given by the difference in the average energies of the initial and final configurations which may be written as $E_i(1s^l 2s^m 2p^n) - E_f(1s^{l+1} 2s^m 2p^{n-1})$.

3.2 *Auger satellite and hypersatellite energies*

For calculation of the energies of Auger satellites and hypersatellites, it may be noted that the transitions are governed only by parity conservation considerations and hence there are many more Auger transitions for a given initial configuration. We may classify these transitions in the following groups: (i) 2*s*–2*s* meaning a 2*s* electron jumps to an initially vacant 1*s* shell and the other 2*s* electron goes to the continuum; (ii) 2*s*–2*p* and (iii) 2*p*–2*p*, with similar meanings. When the K shell is initially doubly ionized, we get the Auger hypersatellite lines.

The energies of the above Auger satellite and hypersatellite lines are given by the difference in the average energies of the following configurations:

(i) For the 2*s*–2*s* Auger lines

$$E_A(2s\text{–}2s) = E_i(1s^l 2s^m 2p^n) - E_f(1s^{l+1} 2s^{m-2} 2p^n),$$

where $m = 2$ and n varies from 1 to 5.
(ii) For the 2*s*–2*p* Auger lines

$$E_A(2s\text{–}2p) = E_i(1s^l 2s^m 2p^n) - E_f(1s^{l+1} 2s^{m-1} 2p^{n-1}).$$

Here if $m = 1$, n takes the values 1 to 6 and if $m = 2$, n takes the values 1 to 5.
(iii) For the 2*p*–2*p* Auger lines

$$E_A(2p\text{–}2p) = E_i(1s^l 2s^m 2p^n) - E_f(1s^{l+1} 2s^m 2p^{n-2}).$$

Here if $m = 0$ and 1, n takes the values 1 to 6, while if $m = 2$, n takes the values 1 to 5. In all the above three cases for the satellites $l = 1$ while for the hypersatellites $l = 0$.

4. Results and discussion

Conventional energy level diagrams for atoms with single vacancies in the K, L_{I}, L_{II}, L_{III} etc shells are well known (Compton and Allison 1963; Agarwal 1979). On the basis of such energy level diagrams, the transitions for the x-ray dipole lines as well as the forbidden lines (Edlabadkar and Mande 1983) can be explained. But energy level diagrams for multiply-ionized atoms, showing the transitions for the x-ray satellite and hypersatellite lines are not available in literature. In the present paper, we have calculated the energies of neon for different electron configurations with more than one hole and made an attempt to draw the energy level diagram (figure 1) for them, taking the energy of the neutral atom as the reference level. In this diagram are shown to scale the energy levels of various electron defect configurations. Such a diagram, to our knowledge, is being given in this work for the first time. We shall now discuss the energy level diagram given in figure 1 at some length.

The energy levels can be divided into three columns *A*, *B* and *C*. The levels in *A* do not have any hole in the 2*s* shell, the levels in B are characterized by a single hole in the 2*s* shell, while the levels in *C* have two holes in the 2*s* shell. The levels in each column may be further divided into three horizontal groups: the lower group (I), the middle group (II) and the upper group (III), where the levels have zero, one and two permanent holes in the *K* shell respectively. Thus the number of holes in the 1*s* and 2*s* shells being fixed in a given subgroup (such as A_{I}, A_{II} etc), the levels in each of them are characterized by increasing the number of holes in the 2*p* shell vertically upwards. It will be seen from figure 1 that the groups I, II and III are not completely separated from each other, but show some overlap.

The x-ray satellite and hypersatellite transitions are indicated in the energy level diagram. They correspond to the 2*p*–1*s* electronic transitions, the electron or hole content of the 2*s* shell being unaffected. Hence they are indicated by vertically downward transitions in each column *A*, *B* and *C*. The x-ray satellites ensuing from a single hole *K* shell configuration are shown as transitions from group II to I in each

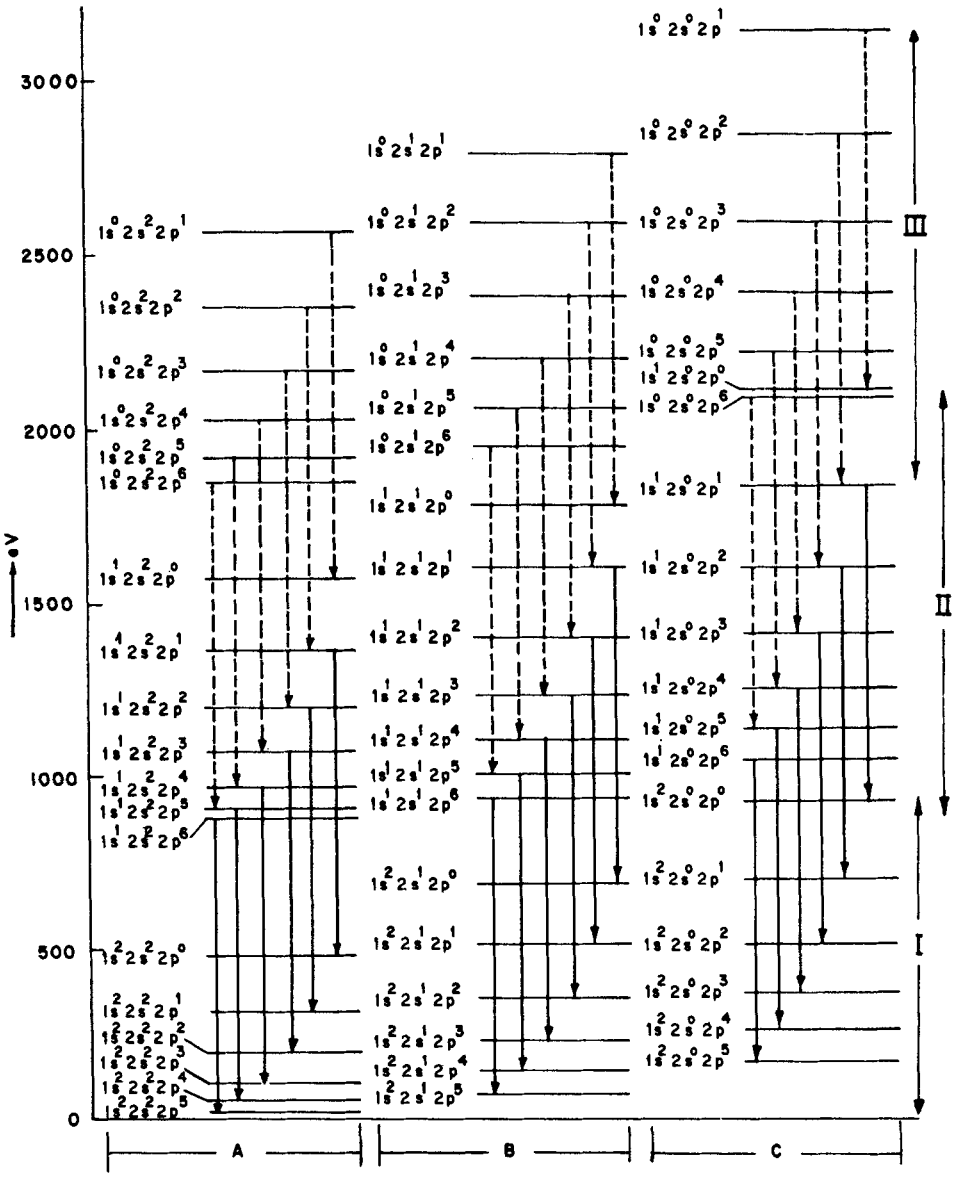

Figure 1. Energy level diagram to scale for the various defect-electron configurations of neon. Continuous vertical lines show x-ray satellite transitions while the broken lines correspond to the hypersatellite transitions.

column, while the hypersatellites which originate in the double hole K shell configuration are shown as vertical transitions from group III to II in each column.

It is interesting to note that even the Auger satellite and hypersatellite transitions can be represented on the energy level diagram given in figure 1. To facilitate the understanding of the Auger transitions, we have redrawn in figure 2 only a few energy levels in the different subgroups of columns A, B and C. Let us first consider the transition $2p$–$2p$. Here as a result of the transition, the holes in the $2p$ shell increase by

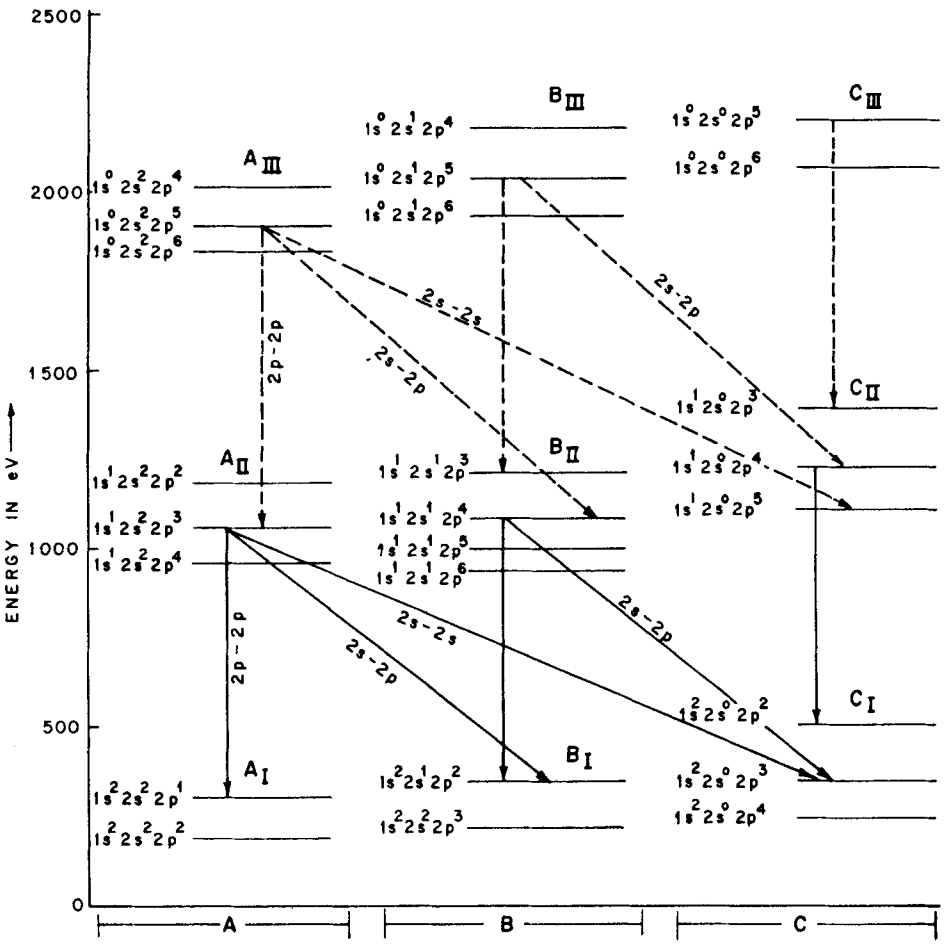

Figure 2. Illustrative partial energy level diagram to scale to show a few Auger satellite and hypersatellite transitions.

two and the hole in 1*s* decreases by one, while the electron/hole content of the 2*s* shell is unaffected. Hence all Auger satellites with 2*p*–2*p* transitions are shown as vertical transitions from A_{II} to A_I or B_{II} to B_I or C_{II} to C_I. The hypersatellites originating from double hole *K* shell configurations are from group III to II in each column. A 2*p*–2*p* Auger transition ensuing from an initial configuration ends on a final configurational level which is just higher than the level where the x-ray transition ensuing from the same level would end. Levels in group II act as initial states for satellites and as final states for hypersatellites of the 2*p*–2*p* Auger transitions. In the case of the 2*s*–2*p* Auger transitions the number of holes in 2*s* and 2*p* increases by one, while that in 1*s* decreases by one. Hence they are shown as cross-transitions between A_{II} and B_I or between B_{II} and C_I for the satellites, and A_{III} to B_{II} or between B_{III} to C_{II} for the hypersatellites. Finally for the 2*s*–2*s* Auger transitions we note that the number of holes in 2*s* increases by two and in 1*s* decreases by one, the electron or hole content of 2*p* being unaffected. Hence these satellites are shown as cross-transitions between the subgroup A_{II} to C_I, while the hypersatellites are shown as transitions between subgroup A_{III} to C_{II}.

The Auger transitions between a higher subshell to an inner subshell of the same major shell of an atom are termed in literature as Coster-Kronig transitions. In the case of neon, they may arise due to transitions between the configurations $1s^l2s^m2p^n$ and $1s^l2s^{m+1}2p^{n-2}$. Here l can take the values 0 to 2, m takes the value 0 and 1 and n any value between 2 and 6. Thus in such transitions, holes in the $2p$ shell increase by two, in $2s$ decrease by 1 and the hole or electron content of the $1s$ shell is unchanged. Thus these Coster-Kronig transitions will take place between a level in B and a level in A or between a level in C and a level in B. The transitions will be horizontal between the subgroups B_1 to A_1 or C_1 to B_1 etc. The Coster-Kronig transitions would take place leftward while the Auger transitions take place rightward. However, we find that the final configurations in all cases of Coster-Kronig transitions is of higher energy than the corresponding initial configurations. Hence we conclude from the diagram that for neon the Coster-Kronig transitions are energetically not possible.

In table 1 we have tabulated our calculated values of the transition energies of the x-ray satellite and hypersatellite lines with all possible initial configurations shown in figure 1. In the same table we have shown the theoretically calculated energies of Bhalla *et al* (1973) who used the HFS model as well as the experimentally measured values of Kauffman *et al* (1973). In most cases there is a fairly close agreement between our values and those of Bhalla *et al*. Similarly, the agreement between our values and the experimental values is quite close, considering the fact that the experimental values involve an error of $\pm$ 2 eV (Kauffman *et al* 1973). In figure 3 are shown the positions of the x-ray satellite and hypersatellite lines as calculated by us, by Bhalla *et al* and those determined experimentally by Kauffman *et al*. It is obvious that there is a dearth of experimentally-determined values and more experiments need to be done to cover the x-ray transitions involving the large number of possible initial configurations of the atom. This is specially so for the lines having high energies.

In tables 2a–2c we have tabulated our calculated transition energies for the Auger satellite and hypersatellite lines arising as a result of the transitions $2p$–$2p$, $2s$–$2p$, and $2s$–$2s$ respectively from different initial electronic configurations for neon. They have been compared with the experimentally measured values of these lines by Matthews *et al* (1973). This comparison has helped us in giving assignments to many of the unassigned lines observed by Matthews *et al*. In the same table we have also tabulated

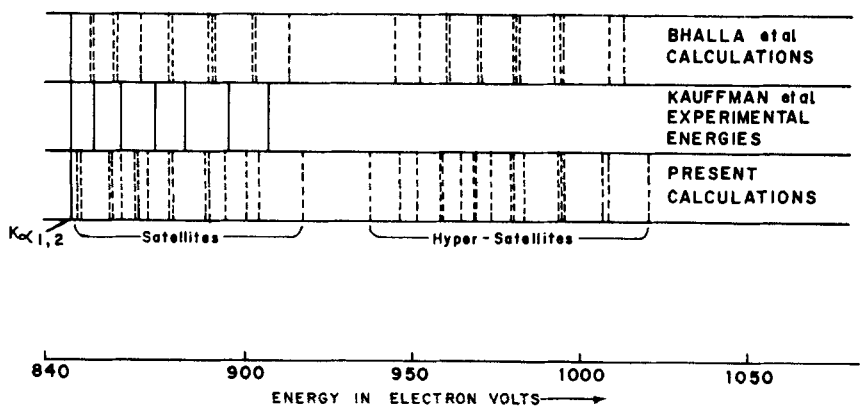

Figure 3. Positions of neon x-ray $K\alpha$ satellite and hypersatellite lines with respect to the $K\alpha$ diagram line.

Table 1. Energies (in eV) of the $K\alpha$ x-ray satellite and hypersatellite lines of neon.

Initial configuration	Present calculations	Experimental energies (Kauffman *et al* 1973)	Calculated values (Bhalla *et al* 1973)
$1s^1 2s^2 2p^6$	846·9	848·0	848·5
Satellites			
$1s^1 2s^2 2p^5$	849·7	855·0	853·7
$1s^1 2s^2 2p^4$	859·6	863·0	860·7
$1s^1 2s^2 2p^3$	867·8	873·0	869·0
$1s^1 2s^2 2p^2$	877·9	882·0	879·0
$1s^1 2s^2 2p^1$	893·8	895·0	890·7
$1s^1 2s^1 2p^6$	851·2		854·6
$1s^1 2s^1 2p^5$	859·3		860·9
$1s^1 2s^1 2p^4$	867·6		868·9
$1s^1 2s^1 2p^3$	877·1		878·5
$1s^1 2s^1 2p^2$	888·8		889·7
$1s^1 2s^1 2p^1$	904·1	907·0	902·6
$1s^1 2s^0 2p^6$	863·2		861·7
$1s^1 2s^0 2p^5$	870·5		869·2
$1s^1 2s^0 2p^4$	878·7		878·3
$1s^1 2s^0 2p^3$	888·2		889·0
$1s^1 2s^0 2p^2$	900·3		901·6
$1s^1 2s^0 2p^1$	916·6	922·0	913·4
Hypersatellites			
$1s^0 2s^2 2p^6$	936·8		945·4
$1s^0 2s^2 2p^5$	945·7		952·3
$1s^0 2s^2 2p^4$	957·5		960·7
$1s^0 2s^2 2p^3$	968·9		970·7
$1s^0 2s^2 2p^2$	980·4		982·3
$1s^0 2s^2 2p^1$	994·5		995·3
$1s^0 2s^1 2p^6$	950·6		952·4
$1s^0 2s^1 2p^5$	958·6		960·4
$1s^0 2s^1 2p^4$	968·2		969·9
$1s^0 2s^1 2p^3$	979·1		980·9
$1s^0 2s^1 2p^2$	992·0		993·5
$1s^0 2s^1 2p^1$	1008·1		1007·6
$1s^0 2s^0 2p^6$	956·1		960·3
$1s^0 2s^0 2p^5$	967·6		969·3
$1s^0 2s^0 2p^4$	983·4		979·9
$1s^0 2s^0 2p^3$	994·4		992·0
$1s^0 2s^0 2p^2$	1006·4		1012·5
$1s^0 2s^0 2p^1$	1020·0		

the theoretically calculated energies of these lines by Bhalla *et al* (1973).

In figures 4 to 7, we have drawn graphs between the energies of the x-ray and Auger satellites and hypersatellites against the increasing number of holes in the $2p$ orbitals. For comparison we have also shown the experimental values of Kauffman *et al* in the x-ray case and of Matthews *et al* in the Auger case. Also shown are the theoretically calculated values of Bhalla *et al*. In these figures *A*, *B* and *C* correspond respectively to the cases of zero, one and two permanent holes in the $2s$ shell. With the progressive increase in the number of holes in the $2p$ shell, the x-ray energies show a regular increase in their values. For the Auger satellites a regular decrease in energy is observed with the

Table 2a. Energies (in eV) of the $K\alpha$ Auger satellites and hypersatellites of neon ($2p$–$2p$ transitions).

Initial configuration	Present Calculations	Experimental energies (Matthews *et al* 1973)	Calculated values (Bhalla *et al* 1973)
$1s^12s^22p^6$	811·4	804·2	807·7
Satellites			
$1s^12s^22p^5$	792·4	790·3	788·2
$1s^12s^22p^4$	770·0	768·8	767·3
		770·7	
$1s^12s^22p^3$	749·0	747·9	745·0
		748·6	
$1s^12s^22p^2$	720·9	720·4	721·4
		722·4	
$1s^12s^12p^6$	796·5	792·1	791·4
$1s^12s^12p^5$	774·1	774·5	770·7
$1s^12s^12p^4$	750·2	748·6	748·6
		749·9	
$1s^12s^12p^3$	726·6	724·3	725·2
$1s^12s^12p^2$	697·3	698·7	700·8
$1s^12s^02p^6$	780·3	780·3	774·5
$1s^12s^02p^5$	754·4	754·4	752·2
$1s^12s^02p^4$	729·4	729·0	729·2
$1s^12s^02p^3$	705·9	702·0	704·9
		703·1	
$1s^12s^02p^2$	678·9	680·4	678·5
		680·7	
Hypersatellites			
$1s^02s^22p^6$	877·3	—	873·0
$1s^02s^22p^5$	858·2	—	850·6
$1s^02s^22p^4$	834·6	—	826·7
$1s^02s^22p^3$	803·2	800·6	801·5
$1s^02s^22p^2$	777·6	776·3	775·0
		777·6	
$1s^02s^12p^6$	858·9	—	854·2
$1s^02s^12p^5$	834·3	—	830·5
$1s^02s^12p^4$	808·0	—	805·4
$1s^02s^12p^3$	781·7	782·1	779·1
		783·1	
$1s^02s^12p^2$	752·3	751·2	751·5
$1s^02s^02p^6$	835·6	—	834·2
$1s^02s^02p^5$	813·0	—	809·4
$1s^02s^02p^4$	784·9	785·5	783·3
$1s^02s^02p^3$	757·6	758·6	756·0
$1s^02s^02p^2$	726·1	729·0	727·2

number of $2p$ holes. For the hypersatellites, with $2p$ holes having a value one or two there is first an increase in energy but as the number of holes increases further, the energy decreases. In all cases, a striking parallelism is observed between the satellite and the hypersatellite lines. That this sort of parallelism exists for the x-ray satellite and hypersatellite lines of magnesium has recently been shown by us (Lakshmi Natarajan *et al* 1986).

Table 2b. Energies (in eV) of the $K\alpha$ Auger satellites and hypersatellites of neon ($2s$–$2p$ transitions).

Initial configuration	Present calculations	Experimental energies (Matthews *et al* 1973)	Calculated values (Bhalla *et al* 1973)
$1s^1 2s^2 2p^6$	777·9	777·6	780·0
Satellites			
$1s^1 2s^2 2p^5$	760·2	758·6	762·8
		759·2	
		761·6	
$1s^1 2s^2 2p^4$	741·2	742·5	744·9
$1s^1 2s^2 2p^3$	728·8	725·1	726·2
$1s^1 2s^2 2p^2$	707·2	708·4	707·0
$1s^1 2s^2 2p^1$	688·1	689·7	687·4
$1s^1 2s^1 2p^6$	761·6	759·2	760·6
		761·6	
$1s^1 2s^1 2p^5$	744·3	744·6	742·6
$1s^1 2s^1 2p^4$	730·6	730·6	723·8
$1s^1 2s^1 2p^3$	710·2	712·5	704·5
		713·0	
$1s^1 2s^1 2p^2$	690·6	692·3	684·8
$1s^1 2s^1 2p^1$	668·7	673·3	663·6
Hypersatellites			
$1s^0 2s^2 2p^6$	852·5	—	847·3
$1s^0 2s^2 2p^5$	831·8	—	828·3
$1s^0 2s^2 2p^4$	811·6	—	808·5
$1s^0 2s^2 2p^3$	786·1	787·5	788·1
		785·5	
$1s^0 2s^2 2p^2$	763·5	764·4	767·1
		765·9	
		766·8	
$1s^0 2s^2 2p^1$	740·2	738·3	745·5
		740·5	
		742·5	
$1s^0 2s^1 2p^6$	829·3	—	825·8
$1s^0 2s^1 2p^5$	807·5	—	805·9
$1s^0 2s^1 2p^4$	786·5	787·5	785·3
		790·3	
$1s^0 2s^1 2p^3$	769·0	766·8	764·2
		768·8	
		770·7	
$1s^0 2s^1 2p^2$	746·0	745·1	742·6
		746·3	
$1s^0 2s^1 2p^1$	718·0	718·4	720·2
		720·4	

It is remarkable to note that, despite the simple model used by us, our calculated values of the transition energies of x-ray as well Auger satellites and hypersatellites are quite close to the experimental and theoretical values of the earlier workers who had used sophisticated HFS wavefunctions. It is well known that the major problem of atomic structure calculations is the treatment of electron-electron interaction, but for the inner shell electrons involved here, the importance of electron-electron interaction is much smaller than the electron-nuclear interaction (Scofield 1975). It is therefore not

Table 2c. Energies (in eV) of the $K\alpha$ Auger satellites and hypersatellites of neon ($2s$–$2s$ transitions).

Initial configuration	Present calculations	Experimental energies (Matthews *et al* 1973)	Calculated values (Bhalla *et al* 1973)
$1s^1 2s^2 2p^6$	749·1	747·9	747·3
		748·6	
		749·9	
		751·2	
Satellites			
$1s^1 2s^2 2p^5$	735·8	735·1	732·1
		736·9	
$1s^1 2s^2 2p^4$	715·9	715·6	716·9
		716·2	
		718·4	
$1s^1 2s^2 2p^3$	700·0	698·7	701·6
		699·5	
		699·9	
		702·0	
$1s^1 2s^2 2p^2$	682·8	684·6	686·4
		686·0	
$1s^1 2s^2 2p^1$	666·4	661·6	671·6
$1s^1 2s^2 2p^0$	652·1	—	—
Hypersatellites			
$1s^0 2s^2 2p^6$	820·1	—	815·7
$1s^0 2s^2 2p^5$	806·6	—	799·9
$1s^0 2s^2 2p^4$	791·5	790·3	784·0
		792·1	
$1s^0 2s^2 2p^3$	775·4	774·5	768·0
		776·3	
		777·6	
$1s^0 2s^2 2p^2$	752·1	751·2	752·3
		754·4	
$1s^0 2s^2 2p^1$	732·6	730·6	736·7
		732·3	
		735·1	
$1s^0 2s^2 2p^0$	702·9	702·0	—
		703·1	

surprising that the simple atomic model used by us gives fairly correct results. This good agreement may also be attributed to the fact that our analytical wavefunctions for the inner shells are in excellent agreement with the HFS wavefunctions of Herman and Skillman (Tankhiwale and Mande 1970).

It may be remarked here that Matthews *et al* attempted to give assignments for only a few Auger satellites while the hypersatellite assignments have not been attempted by them at all. It will perhaps not be inappropriate to offer some comments (given in table 3) on their assignments.

Woods *et al* (1975) reported in F^{9+} + Ne bombardment experiments, the emission of a group of unresolved Auger lines from Ne at 110 eV above the ^1D diagram line, that is at about 917 eV. They account for this line as arising from transitions involving a double K shell vacancy in neon in the initial state, indicating that it is a hypersatellite.

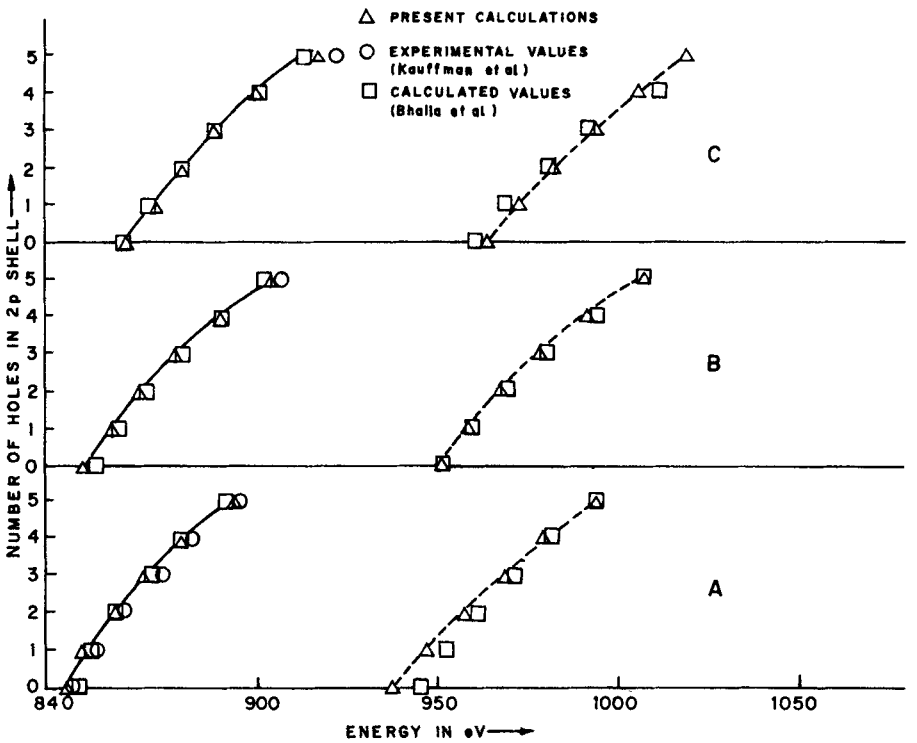

Figure 4. Variation of the energies of the x-ray satellite lines (continuous curves) and hypersatellite lines (dotted curves) with number of holes in the $2p$ shell. A, B and C respectively denote atoms with no permanent holes, one and two permanent holes in the $2s$ shell.

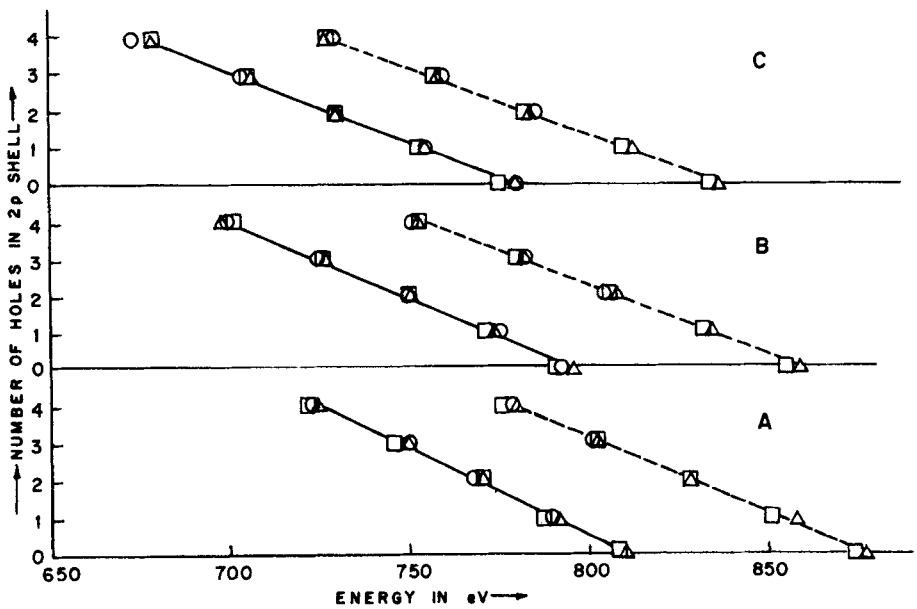

Figure 5. Variation of the energies of neon Auger satellite (continuous curves) and hypersatellite lines (broken curves) with the number of holes in the $2p$ shell, for the $2p$–$2p$ transitions. A, B and C respectively denote atoms with no permanent holes, one and two permanent holes in the $2s$ shell. Key to symbols as given in figure 4.

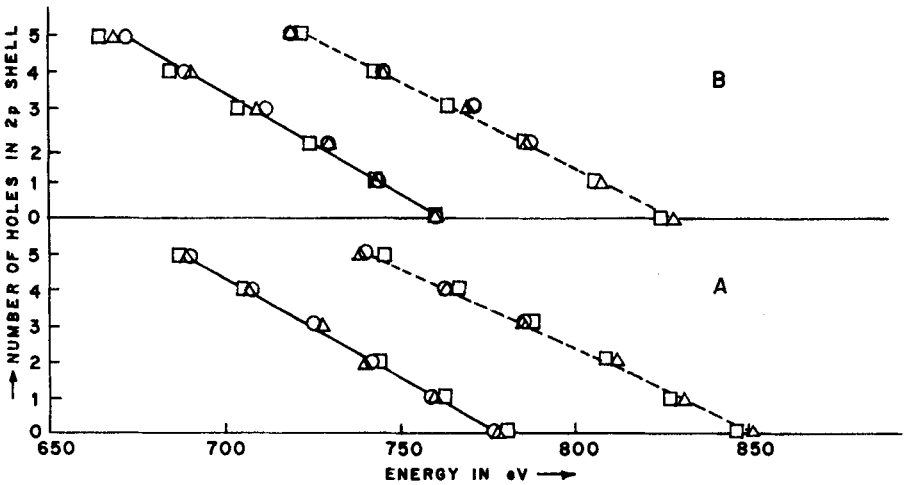

Figure 6. Variation of the energies of neon Auger satellite (continuous curves) and hypersatellite lines (broken curves) with the number of holes in the 2*p* shell for the 2*s*–2*p* transitions. A and B denote atoms with no permanent hole and one permanent hole respectively in the 2*s* shell. Key to symbols as given in figure 4.

Table 3. Comments on the assignments of satellites and hypersatellites in Auger spectra.

Data given by Matthews *et al* (1973)			
Line number	Energy in eV	Assignment	Our comments
1	661·3	111*pp*	With just one electron in the 2*p* shell in the initial state, it is difficult to understand how a *p*–*p* transition can occur. We feel that this line corresponds to the 121*ss* transition for which our calculated energy is 666·4 eV.
13	702·0	123*ss*	The whole group from line number 10 to 13 can be given the assignment 123*ss*. An alternative assignment 020*ss* is also possible for these lines.
26	730·6	125*ss*	The group from 26 to 29 could be given the assignment 021*ss* in addition to 125*ss*.
	732·3		
	735·1		
29	736·9	124*sp*	
44	761·6	114*pp*	The theoretically calculated values for the transition 114*pp* being 750·2 eV, this assignment appears to be incorrect. On the contrary, the lines 42, 43 and 44 with energies 758·6, 759·2 and 761·6 respectively should have the assignment 125*sp*.
52	774·5	124*pp*	The assignment should be 115*pp*, the calculated energy being 774·1 eV.
57	783·1	125*pp*	The assignment should be 004*pp*, the calculated energy being 784·9 eV.
58	785·5	125*pp*	The assignment should be 023*sp*, the calculated energy being 786·1 eV.
59	787·5	125*pp*	The assignment should be 014*sp*, the calculated energy being 786·5 eV.
62	800·6	126*pp*	The assignment should be 023*pp*, the calculated energy being 803·2 eV.

As an example of the notation the transition 123*ss* means that the transition is from the initial configuration $1s^1 2s^2 2p^3$ in the 2*s*-2*s* series.

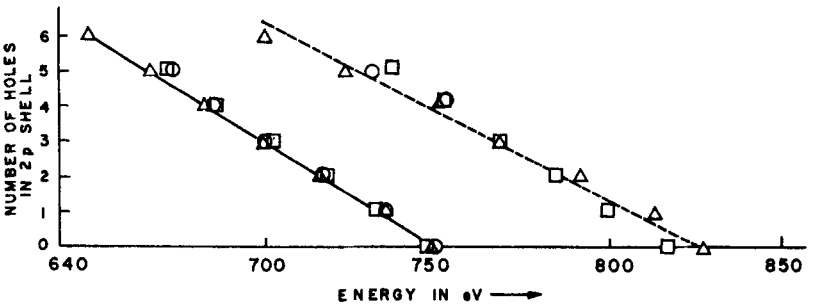

Figure 7. Variation of the energies of neon Auger satellite (continuous curves) and hypersatellite lines (dotted curves) with the number of holes in the $2p$ shell for the $2s$–$2s$ transitions. Key to symbols as given in figure 4.

Our theoretical calculations give the maximum energy of the hypersatellites of neon as 877·3 eV while the calculations of Bhalla *et al* give 873·0 eV as the upper limit for the hypersatellites. Hence this observed line at 917·7 eV cannot be a hypersatellite of neon. It might probably be arising due to the emission from additional electronic levels of the pseudo-molecules formed (Fano and Lichten 1965) in the $F^{9+} + Ne$ collisions.

Our work thus brings out the need for a more detailed experimentation on satellites and hypersatellites in Auger spectra. Matthews *et al* report in their paper the possibility of occurrence of about 150–190 Auger satellite lines. These can of course be accounted for, if in the LS coupling approximation, the multiplet structures arising in the concerned initial and the final configurations are taken into account. In the present calculations as well as those of Bhalla *et al* these multiplet structures have been overlooked. However, at the present state of art of Auger spectroscopy it seems very difficult to resolve the multiplet structures, as has been remarked by Matthews *et al*.

5. Concluding remarks

We have shown in this paper how the energies of the satellite and hypersatellite lines in the x-ray and Auger spectra of a light element like neon can be calculated, making use of screened hydrogenic wavefunctions. Our method, although relatively simple, leads to an understanding of the ionization processes in the inner shells of atoms and gives a picture of all possible transient multiply-ionized states. From the energy level diagram drawn by us for the various defect electron configurations of neon, it becomes evident that the Coster-Kronig transitions are not energetically possible for neon. It has not been possible for us to calculate the transition rates for the satellite and hypersatellite lines. We propose to undertake such calculations in the near future. Our theoretical work nevertheless shows that it is now necessary to carry out more detailed experiments on the satellites and hypersatellites in x-ray and Auger spectra. With the high energy ion bombarding facilities now available, it should be possible to carry out such studies which would considerably add to our knowledge of atomic configurations.

References

Åberg T 1967 *Phys. Rev.* **156** 35

Åberg T and Suvanen M 1982 *Advances in x-ray spectroscopy* (eds) C Bonnelle and C Mande (New York: Pergamon Press) Ch. 1

Agarwal B K 1979 *X-ray spectroscopy – An introduction; Springer series in optical sciences* (eds) D L Mac Adam, Vol. 15
Bambynek W, Crasemann B, Fink R W, Freund H U, Mark H, Swift C D, Price R E and Rao P V 1972 *Rev. Mod. Phys.* **44** 716
Bhalla C P, Folland N O and Hein M A 1973 *Phys. Rev.* **A8** 649
Briand J P, Chevallier P M, Tavernier M and Rozet J P 1971 *Phys. Rev. Lett.* **27** 777
Burch D, Ingalls W B, Risley J S and Heffner R 1972 *Phys. Rev. Lett.* **29** 1719
Burch D 1973 in *Proc. Int. Conf. Phys. Electron. At. Collisions*, 8th Belgrade, Yugoslavia
Burhop E H S and Asaad W N 1972 *Advances in atomic and molecular physics* (ed.) D R Bates (New York: Academic Press) Vol. 8
Carlson T A, Nestor C W, Tucker T C and Malik F B 1968 *Phys. Rev.* **169** 27
Compton A H and Allison S K 1963 *X-rays in theory and experiment* (New York: Van Nostrand)
Condon E U and Shortley G H 1977 *Theory of atomic spectra* (Cambridge: University Press)
Crasemann B 1975 *Atomic inner shell processes* (New York: Academic Press) Vol. 1
Deodhar G B 1962 *Proc. Natl. Acad. Sci. India* **A32** 320
Edlabadkar V S and Mande C 1983 *Pramana (J. Phys.)* **20** 175
Emery G T 1975 *Atomic inner shell processes* (New York: Academic Press) Vol. 1 p. 201
Fano U and Lichten W 1965 *Phys. Rev. Lett.* **14** 627
Fink R W, Manson S T, Palms J M and Rao P V (eds) 1973 *Proc. Int. Conf. Inn. Shell Ioniz. Phenomena Future Appli.*, Atlanta, U.S. At. Energy Comm. Rep. No. CONF 720404, Oak Ridge, Tennessee
Garcia J D, Fortner R J and Kavanagh T M 1973 *Rev. Mod. Phys.* **45** 111
Herman F and Skillman S 1963 *Atomic structure calculations* (New Jersey: Prentice-Hall) Ch. 6
Hirsch F R 1942 *Rev. Mod. Phys.* **14** 45
Kauffman R L, Hopkins F F, Woods C W and Richard P 1973 *Phys. Rev. Lett.* **31** 621
Kothari D S and Majumdar R C 1929 *Z. Phys.* **61** 712
Krause M O 1973 *Proc. Int. Conf. Inn. Shell Ioniz. Phenomena Future Appli.*, Atlanta, US At. Energy Comm. Rep. No. CON F 720404, Oak Ridge, Tennessee
Krause M O, Steview F A, Lewis L J, Carlson T A and Moddeman W E 1970 *Phys. Lett.* **A31** 81
Lakshmi Natarajan, Tankhiwale A V and Mande C 1986 *Pramana (J. Phys.)* **26** 55
Larkins F P 1971a *J. Phys.* **B4** 1
Larkins F P 1971b *J. Phys.* **B4** 14
Matthews D L, Johnson B M, Mackey J J and Moore C F 1973 *Phys. Rev. Lett.* **31** 1331
McGuire F J 1975 *Atomic inner shell processes* (ed) B Crasemann (New York: Academic Press) Vol. 1 p. 293
Morse P M, Young L A and Haurwitz E 1935 *Phys. Rev.* **48** 948
Ogurtsov G N 1972 *Rev. Mod. Phys.* **44** 1
Richard P, Hodge W and Moore C F 1973 *Phys. Rev.* **7** 1437
Richard P 1975 *Atomic inner shell processes* (ed) B Crasemann (New York: Academic Press) Vol. 1 p. 73
Rudd M E and Macek J H 1972 *Case Stud. At. Phys.* **3** No. 2
Sachenko V P and Demekhin V F 1966 *Sov. Phys. JETP* **22** 532
Sagawa T 1971 *J. Phys. (Paris)* **32 C4** 186
Saha M N 1920 *Philos. Mag.* **40** 472, 809
Saha M N 1921 *Proc. Roy Soc. (London)* **A99** 135
Saha M N and Banerji A C 1931 *Z. Phys.* **68** 704
Scofield J H 1975 *Atomic inner shell processes* (ed) B Crasemann (New York: Academic Press) Vol. 1 p. 265
Siegbahn 1925 *The spectroscopy of x-rays* (Oxford: University Press)
Slater J C 1960 *Quantum theory of atomic structure* (New York: McGraw Hill) Vol. 1
Tankhiwale A V and Mande C 1970 *J. Phys.* **B3** 774
Tankhiwale A V, Khare P L and Mande C 1971 *J. Phys.* **B4** 1250
Woods C W, Kauffman R L, Jamison K A, Stolterfoht N and Richard P 1975 *Int. Conf. on physics of electronic and atomic collisions*, Washington: Seattle p. 417